

Article

Reactive Hydride Composite of Mg_2NiH_4 with Borohydrides Eutectic Mixtures

Erika M. Dematteis ^{1,2} , Silvère Vaunois ^{1,3}, Claudio Pistidda ² , Martin Dornheim ² and Marcello Baricco ^{1,*} 

¹ Department of Chemistry and Inter-Departmental Center Nanostructured Interfaces and Surfaces (NIS), University of Turin, Via Pietro Giuria 7, 10125 Torino, Italy; erikamichela.dematteis@unito.it (E.M.D.); silvere.vaunois@gmail.com (S.V.)

² Nanotechnology Department, Helmholtz-Zentrum Geesthacht Max-Planck Straße 1, 21502 Geesthacht, Germany; claudio.pistidda@hzg.de (C.P.); martin.dornheim@hzg.de (M.D.)

³ Laboratoire de Cristallographie et Sciences des Matériaux (CRISMAT), UMR 6508, Normandie University, ENSICAEN, UNICAEN, CNRS, 14000 Caen, France

* Correspondence: marcello.baricco@unito.it; Tel.: +39-011-6707569

Received: 20 January 2018; Accepted: 7 February 2018; Published: 10 February 2018

Abstract: The development of materials showing hydrogen sorption reactions close to room temperature and ambient pressure will promote the use of hydrogen as energy carrier for mobile and stationary large-scale applications. In the present study, in order to reduce the thermodynamic stability of MgH_2 , Ni has been added to form Mg_2NiH_4 , which has been mixed with various borohydrides to further tune hydrogen release reactions. De-hydrogenation/re-hydrogenation properties of $\text{Mg}_2\text{NiH}_4\text{-LiBH}_4\text{-M}(\text{BH}_4)_x$ ($\text{M} = \text{Na}, \text{K}, \text{Mg}, \text{Ca}$) systems have been investigated. Mixtures of borohydrides have been selected to form eutectics, which provide a liquid phase at low temperatures, from 110 °C up to 216 °C. The presence of a liquid borohydride phase decreases the temperature of hydrogen release of Mg_2NiH_4 but only slight differences have been detected by changing the borohydrides in the eutectic mixture.

Keywords: eutectic; borohydride; reactive hydride composite; hydrogen storage

1. Introduction

To overcome the increasing worldwide demand of energy, the use of hydrogen as sustainable and efficient energy carrier plays an essential role. In this frame, the development of materials able to store hydrogen close to room temperature and ambient pressure will enable the use of hydrogen in mobile and stationary large-scale applications. Low cost and light weight hydrides are promising materials for solid-state hydrogen storage, owing to their high gravimetric and volumetric hydrogen capacity [1]. The theoretical hydrogen content of LiBH_4 is 18.5% wt, i.e., the highest among metal borohydrides, while it is equal to 10.7% wt for NaBH_4 , 7.5% wt for KBH_4 , 14.9% wt for $\text{Mg}(\text{BH}_4)_2$ and 11.6% wt for $\text{Ca}(\text{BH}_4)_2$. Observed values are usually lower, depending on the experimental conditions.

Usually light metal hydrides absorb and release hydrogen through sluggish kinetics at relatively high temperatures. In order to reduce their thermodynamic stabilities, transition metals have been added to form complex metal hydrides [2], such as in the case of MgH_2 mixed with Ni to form Mg_2NiH_4 , with a theoretical hydrogen content equal to 3.6% wt. This complex metal hydride, upon heating, shows a polymorphic transition from a monoclinic to a cubic structure at 244 °C, together with the release of one hydrogen to form Mg_2NiH_3 [3,4]. The main dehydrogenation reaction occurs at 305 °C under 5% H_2 /95% N_2 flow or 1 bar H_2 [3,5]. The thermodynamic properties of the Mg-Ni-H ternary system were assessed by Zeng et al. [6], where the values of temperature of decomposition as a function of hydrogen pressure are reported. Upon cycling at low hydrogen pressure, Mg_2Ni can

absorb hydrogen (at $T_{\text{peak}} = 247\text{ }^{\circ}\text{C}$, at 3 bar H_2) to form the partial hydrogenated hexagonal solid solution $\text{Mg}_2\text{NiH}_{0.3}$ [7].

Borohydrides are a class of inorganic ionic materials suitable for hydrogen storage in the solid state [8]. The most promising ones contain a light alkali or alkali-earth metal cation ionically bonded to the complex borohydride anion (BH_4^-) [8]. They attracted the attention of the latest research thanks to their extremely rich chemistry and tuneable properties in relation to their structures and interactions in mixtures. Among borohydrides, several bimetallic compounds are present. Moreover, selected mixtures of borohydrides form eutectic melts at a relatively low temperatures [9]. This feature can be used to easily infiltrate them in nanometric scaffold to improve the hydrogen absorption/desorption kinetics and cyclability [10]. Recently, a systematic study of hydrogen release in pure and eutectic mixtures of borohydrides was reported by Paskevicius et al. [9].

The full understanding of thermodynamic and kinetic properties of hydrogen sorption in borohydride-based systems will allow obtaining new suitable materials for effective hydrogen storage. In the literature, many tailoring routes have been proposed to improve thermodynamic and kinetic properties of both metal hydrides and complex hydrides. The so called Reactive Hydride Composites (RHC), for example, allow mixtures of metal hydrides and borohydrides to release hydrogen in a reversible manner under moderate temperature and hydrogen pressure conditions [11].

The thermodynamic properties and phase diagrams of the $\text{LiBH}_4\text{-NaBH}_4\text{-KBH}_4$ system were recently assessed [12]. In this system, two eutectic compositions are present. $0.725\text{LiBH}_4\text{-}0.275\text{KBH}_4$ (LiK) and $0.70\text{LiBH}_4\text{-}0.30\text{NaBH}_4$ (LiNa) melt at an onset temperature of $105\text{ }^{\circ}\text{C}$ and $216\text{ }^{\circ}\text{C}$, respectively. Even if the LiK eutectic shows a stable liquid above $105\text{ }^{\circ}\text{C}$, it does not decompose below $400\text{ }^{\circ}\text{C}$ [13]. The decomposition of the $0.68\text{LiBH}_4\text{-}0.32\text{NaBH}_4$ mixture was investigated in the literature and it shows a release above $400\text{ }^{\circ}\text{C}$ [14], lowered to $250\text{ }^{\circ}\text{C}$ when nanoconfined [15]. $0.55\text{LiBH}_4\text{-}0.45\text{Mg}(\text{BH}_4)_2$ eutectic composition (LiMg) melts at $180\text{ }^{\circ}\text{C}$ and releases hydrogen during melting and above $250\text{ }^{\circ}\text{C}$ [16–18], its decomposition is lowered to $150\text{ }^{\circ}\text{C}$ upon nanoconfinement, thus suppressing the evolution of diborane and the formation of closoboranes [19,20]. $0.68\text{LiBH}_4\text{-}0.32\text{Ca}(\text{BH}_4)_2$ eutectic composition (LiCa) melts at $200\text{ }^{\circ}\text{C}$ and decomposes at $350\text{ }^{\circ}\text{C}$ [21], lowered down to $200\text{ }^{\circ}\text{C}$ upon confinement [22–25].

Recently various studies have explored the hydrogen release properties of mixtures of complex metal hydrides and borohydrides, such in the case of $\text{Mg}_2\text{FeH}_6\text{-M}(\text{BH}_4)_x$ systems ($\text{M} = \text{Li, Na, K, Mg, Ca}$) [26]. $\text{Mg}_2\text{NiH}_4\text{-M}(\text{BH}_4)_x$ systems ($\text{M} = \text{Li, Na, Ca}$) have been studied as well, showing an improvement of the hydrogen release properties and cyclability [27–31]. The decomposition reactions can form boride species (e.g., $\text{MgNi}_{2.5}\text{B}_2$), which reversibly play as B-donors to form back the borohydride during the re-hydrogenation process. In the $\text{Mg}_2\text{NiH}_4\text{-LiBH}_4$ system, hydrogen release under argon flow starts at roughly $300\text{ }^{\circ}\text{C}$ and it can be re-hydrogenated at 100 bar and $350\text{ }^{\circ}\text{C}$ in about 4 h [27]. The hydrogen release in the $\text{Mg}_2\text{NiH}_4\text{-NaBH}_4$ system has an onset temperature close to $250\text{ }^{\circ}\text{C}$ under vacuum and it occurs in three different steps [29]. The $\text{Mg}_2\text{NiH}_4\text{-Ca}(\text{BH}_4)_2$ system releases hydrogen above $300\text{ }^{\circ}\text{C}$ [30]. There is no report in the literature on the $\text{Mg}_2\text{NiH}_4\text{-KBH}_4$ system, since it is expected to release hydrogen at temperatures that are considered not suitable for the employment of this material in real applications. The $\text{Mg}_2\text{NiH}_4\text{-Mg}(\text{BH}_4)_2$ system has not been studied yet.

As reported above, mixtures of borohydrides have shown the formation of eutectic melts, which allow the release of hydrogen from the liquid state at low temperatures [13,32]. In the present study, we apply the RHC approach to eutectic mixtures of borohydrides, aiming to further improve hydrogen sorption properties of the mixed borohydrides. In order to compare our results with the literature, we investigated the as prepared Mg_2NiH_4 and the RHC mixture $\text{Mg}_2\text{NiH}_4\text{-LiBH}_4$. Then Mg_2NiH_4 was mixed with all the binary eutectic compositions of LiBH_4 and $\text{M}(\text{BH}_4)_x$ ($\text{M} = \text{Na, K, Mg, Ca}$). The thermal behaviour and decomposition temperature were analysed by High-Pressure Differential Scanning Calorimetry (HP-DSC). Ball milled mixtures (BM) and samples after thermal cycling were analysed by powder X-ray diffraction (PXRD) to identify crystalline decomposition products. This study

will allow an understanding of the behaviour of a RHC mixtures with a liquid phase and its role in the thermodynamic destabilization of hydrogen sorption reactions.

2. Materials and Methods

Mg₂NiH₄ was synthesized by ball milling (BM) MgH₂ and Ni in a molar ratio 2:1. Approximately 5 g of powder were milled in a planetary Fritsch Pulverisette 6 mill for 10 h at 350 r.p.m. in a custom-made stainless steel (SS) 250 mL vial, under 10 bar of hydrogen and a ball-to-powder mass ratio of 5:1, using 15 mm SS balls. After milling, the powder was transferred in a Parr Reactor and heated under 10 bar of hydrogen up to 370 °C for 10 h.

Lithium borohydride (LiBH₄, purity >99% from Rockwood Lithium), sodium borohydride (NaBH₄, purity 99.99% from Sigma-Aldrich), potassium borohydride (KBH₄, purity 99% from Sigma-Aldrich), magnesium borohydride (Mg(BH₄)₂, purity >95% from KatChem) and calcium borohydride (Ca(BH₄)₂, purity >95% from KatChem) were mixed by BM in the eutectic molar composition. Approximately 1 g of sample was milled under nitrogen atmosphere in 80 mL SS vials and with SS balls (o.d. 5 mm), with a balls-to-powder mass ratio of 30:1. The samples were milled at 350 r.p.m. for 5 min for 12 times, with a 2 min pause in between each run. Using the same BM settings, the eutectic borohydride mixtures and Mg₂NiH₄ were ball milled together in the correct molar ratio to obtain a complete conversion to MgNi_{2.5}B₂ after decomposition of the borohydrides. All preparations and manipulations of the samples were performed in an argon or nitrogen-filled glove box with a circulation purifier, *p*(O₂, H₂O) < 1 ppm. An overview of milled samples and corresponding compositions is reported in Table 1. The investigated mixtures will be named by the main metals that are present (e.g., the LiBH₄ and KBH₄ in eutectic composition will be named LiK and its mixture with Mg₂NiH₄ will be named MgNiLiK).

Table 1. Investigated samples and their molar composition.

Sample	Borohydrides Composition (Molar Fraction)	RHC Composition (Molar Fraction)
MgNiLi	LiBH ₄	0.56 Mg ₂ NiH ₄ , 0.44 LiBH ₄
MgNiLiK	0.72 LiBH ₄ , 0.28 KBH ₄	0.56 Mg ₂ NiH ₄ , 0.32 LiBH ₄ , 0.12 KBH ₄
MgNiLiNa	0.70 LiBH ₄ , 0.30 NaBH ₄	0.56 Mg ₂ NiH ₄ , 0.31 LiBH ₄ , 0.13 NaBH ₄
MgNiLiMg	0.55 LiBH ₄ , 0.45 Mg(BH ₄) ₂	0.64 Mg ₂ NiH ₄ , 0.20 LiBH ₄ , 0.16 Mg(BH ₄) ₂
MgNiLiCa	0.68 LiBH ₄ , 0.32 Ca(BH ₄) ₂	0.62 Mg ₂ NiH ₄ , 0.27 LiBH ₄ , 0.11 Ca(BH ₄) ₂

To analyse the phase mixtures and decomposition products, powder X-ray diffraction (PXRD) measurements were performed at room temperature. A Panalytical X-pert (Almelo, The Netherlands) (Cu K_α = 1.54059 Å, K_β = 1.54446 Å; K_α/K_β = 0.375) in capillary transmission set-up (Debye-Scherrer geometry) was used. Patterns were collected from 10° to 70° 2θ range, step size 0.016, time step 60 s. Samples were mounted in the glove box in 0.5 mm glass capillaries and sealed with plastiline, then moved out of the glove box and sealed with flame.

To analyse hydrogen release and thermal behaviour of the samples, approximately 5 mg of powder were loaded into aluminium crucibles with a lid, where a hole was made to let the gas flow out. A high-pressure 204 Netsch DSC (HP-DSC, NETZSCH GmbH, Selb, Germany), inside a nitrogen-filled glove box, was used to analyse all the samples. Heating and cooling were performed from room temperature (RT) up to 440 °C at 5 °C/min under a static pressure of 2.2 bar of H₂ loaded at RT, that rose up to 2.8 bar at 440 °C. To clarify reversibility and phase transformation various cycling were performed.

3. Results

Figures 1a, 2a, 3a, 4a, 5a and 6a, report PXD patterns of the as-prepared samples, which can be compared with the patterns collected after thermal cycling. Figures 1b, 2b, 3b, 4b, 5b and 6b show the DSC traces upon cycling.

3.1. Mg_2NiH_4

As a consequence of the synthesis procedure, the diffraction pattern of Mg_2NiH_4 (Figure 1a, as synthesized) presents broad diffraction peaks of the monoclinic phase stable at room temperature, LT1. The orange-reddish colour of the powder indicates the presence of a microtwinned modification of the room-temperature phase, called LT2 [33], as confirmed by PXD pattern. As previously reported for a similar synthesis route [34], even if a molar ratio 2:1 of starting MgH_2 and Ni have been used to obtain the complex metal hydride, traces of unreacted Ni are present in the sample.

In the DSC trace of pure Mg_2NiH_4 on heating (Figure 1b, 1st cycle), at $T_{peak} = 244$ °C, the monoclinic-to-cubic polymorphic phase transition can be observed. This transition is reversible, as clearly shown by the exothermic peak upon cooling at $T_{peak} = 234$ °C, due to the cubic high temperature phase forming LT1 and LT2 [3,4]. In the 2nd cycle (Figure 1b, 2nd cycle), the polymorphic transition is observed again and upon further heating an endothermic peak related to hydrogen release can be detected. The complex metal hydride decompose to Mg_2Ni [34], under a hydrogen backpressure of 2.7 bar, at $T_{peak} = 372$ °C. Upon cooling, in the 2nd cycle, a broad exothermic peak of hydrogenation to form $Mg_2NiH_{0.3}$ can be observed below 235 °C [7]. Upon further cycling (Figure 1b, 3rd cycle), the sample releases hydrogen starting from 280 °C ($T_{peak} = 296$ °C), from $Mg_2NiH_{0.3}$.

$Mg_2NiH_{0.3}$, together with traces of Mg_2NiH_4 , is observed in PXD after cooling (Figure 1a, after DSC).

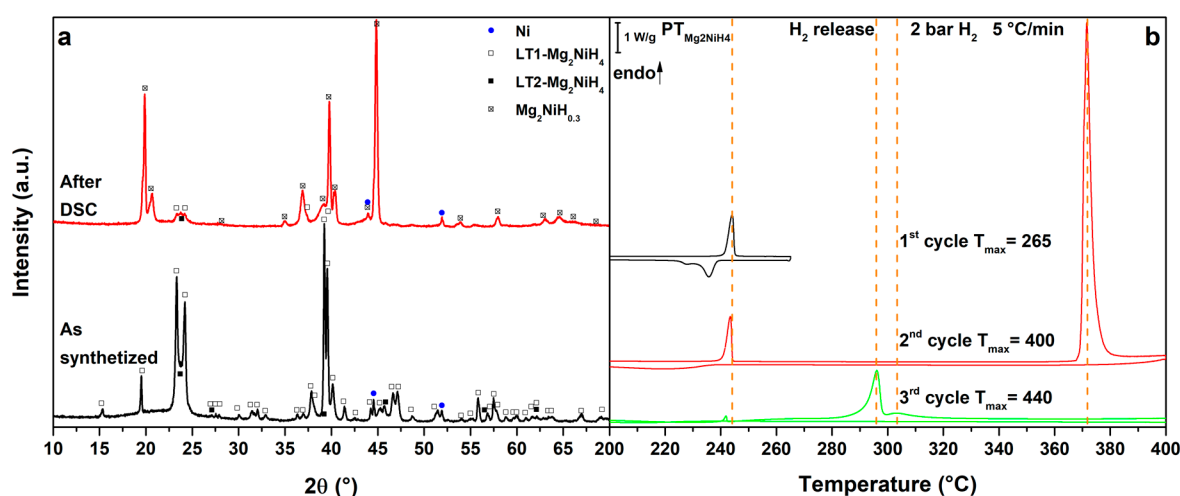


Figure 1. (a) PXD of the as synthesized Mg_2NiH_4 (black, down) and after cycling in HP-DSC (red, up); (b) HP-DSC cycling of Mg_2NiH_4 at 5 °C/min under a static pressure of 2.2 bar of H_2 .

3.2. RHC Mixtures

In almost all the diffraction patterns of Mg_2NiH_4 mixed with borohydrides, the composing phases are visible (Figures 2a, 3a, 4a, 5a and 6a, BM). However, in the $MgNiLiK$ system (Figure 3a, BM), the milling causes the formation of the $LiK(BH_4)_2$ bimetallic phase, in agreement with the literature [32]. In the $MgNiLiMg$ system (Figure 5a, BM), $LiBH_4$ and $Mg(BH_4)_2$ are hardly visible after milling.

3.3. Mg_2NiH_4 - $LiBH_4$

Figure 2b shows the DSC signals for the RHC mixture $MgNiLi$ upon cycling. In the 1st cycle (Figure 2b, 1st cycle), the polymorphic transition of $LiBH_4$ is identified $T_{peak} = 117^\circ C$, which is reversible upon cooling. In the 2nd cycle (Figure 2b, 2nd cycle), after the polymorphic transition of $LiBH_4$, also the polymorphic phase transition of Mg_2NiH_4 is observed as a broad peak around $245^\circ C$. Both DSC signals can be observed also on cooling. Furthermore, in the 3rd cycle (Figure 2b, 3rd cycle), after the polymorphic transition peaks, the melting of $LiBH_4$ can be detected at $T_{peak} = 279^\circ C$. All transitions are reversible and well visible during the cooling process and temperature values are in good agreement with the literature [3,4,35]. In the 4th cycle (Figure 2b, 4th cycle), after the polymorphic transition peaks and $LiBH_4$ melting, at $T_{peak} = 308^\circ C$ a broad endothermic peak due to hydrogen release from $LiBH_4$ can be observed under 2.7 bar H_2 . In this case, on cooling, only small peaks from the polymorphic transitions can be observed, suggesting the occurrence of a reaction. In fact, in the last cycle (Figure 2b, 5th cycle) only small DSC peaks of Mg_2NiH_4 polymorphic transition, $LiBH_4$ polymorphic transition and melting can be observed on heating, evidencing the presence of a small quantity of parent hydrides in the sample. At higher temperatures, at $T_{peak} = 335^\circ C$, the main hydrogen release from the RHC mixture can be observed, with $LiBH_4$ and Mg_2NiH_4 forming $MgNi_{2.5}B_2$ and Mg . Upon cooling below $307^\circ C$, Mg absorbs hydrogen to form MgH_2 .

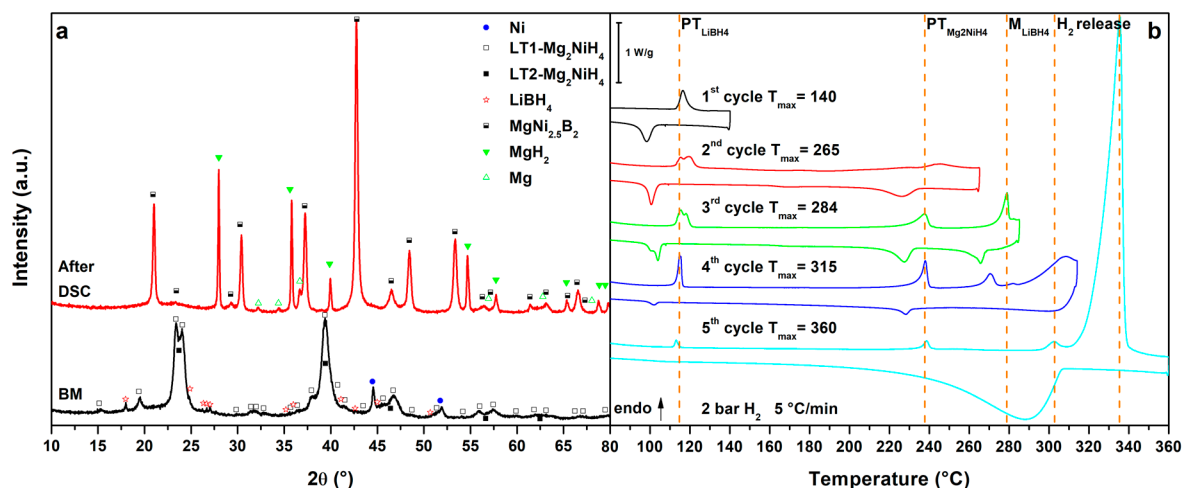


Figure 2. (a) PXD of the ball milled $MgNiLi$ system (black, down) and after cycling in HP-DSC (red, up); (b) HP-DSC cycling of $MgNiLi$ at $5^\circ C/min$ under a static pressure of 2.2 bar of H_2 .

The PXD pattern after the DSC analysis (Figure 2a, after DSC) confirms the total decomposition of $LiBH_4$ and Mg_2NiH_4 . In fact, $MgNi_{2.5}B_2$, MgH_2 and a small quantity of unreacted Mg are observed but no Li-containing phases are evidenced, likely because of the light scattering factor. $LiBH_4$ cannot be reformed because of the low hydrogen pressure applied. The obtained results are in good agreement with the literature [27] and confirms the decrease of the decomposition temperature of both Mg_2NiH_4 and $LiBH_4$ when mixed together into a RHC.

3.4. Mg_2NiH_4 - $LiBH_4$ - KBH_4 Eutectic Composition

Figure 3 reports the results obtained for the $MgNiLiK$ system. Upon heating, in the 1st cycle (Figure 3b, 1st cycle), the melting of the LiK eutectic can be observed at $T_{peak} = 110^\circ C$, which is reversible upon cooling [12]. In the 2nd cycle (Figure 3b, 2nd cycle), after the eutectic melting, the polymorphic transition of Mg_2NiH_4 is observed as a broad peak at $T_{peak} = 246^\circ C$. Above $290^\circ C$ ($T_{peak} = 325^\circ C$) the main hydrogen release from the RHC mixture can be observed under 2.7 bar H_2 . The mixture has decomposed into $MgNi_{2.5}B_2$, Mg_2Ni and Mg . In fact, a broad peak of hydrogenation

can be detected, upon cooling, below 300 °C to form $\text{Mg}_2\text{NiH}_{0.3}$ and MgH_2 . In the 3rd cycle (Figure 3b, 3rd cycle), no transitions from LiK eutectic and Mg_2NiH_4 are observed, endorsing their decomposition. Hydrogen release is observed in a broad peak around 292 °C, related to the hydrogen release from $\text{Mg}_2\text{NiH}_{0.3}$ and above 310 °C, related to decomposition of MgH_2 . In this case, the hydrogen release temperature of the RHC mixture is lower of about 10 °C compared to the MgNiLi system. Upon cooling, the Mg hydrogenation peak is more defined in the 3rd cycle because of a possible activation upon previous thermal cycling.

$\text{Mg}_2\text{NiH}_{0.3}$, MgH_2 and $\text{MgNi}_{2.5}\text{B}_2$ are present in the PXD pattern after DSC (Figure 3a, after DSC), together with an unknown phase. The XRD peak positions of this unknown phase correspond to those observed after decomposition of the $\text{Mg}_2\text{NiH}_4\text{-Ca}(\text{BH}_4)_2$ system [30]. The presence of KBH_4 in the mixture suggests that not all the borohydride present in the mixture has been decomposed upon thermal cycling. Therefore, from the liquid eutectic mixture of borohydrides, only LiBH_4 actively reacts with Mg_2NiH_4 , whereas the most stable KBH_4 remains unaffected.

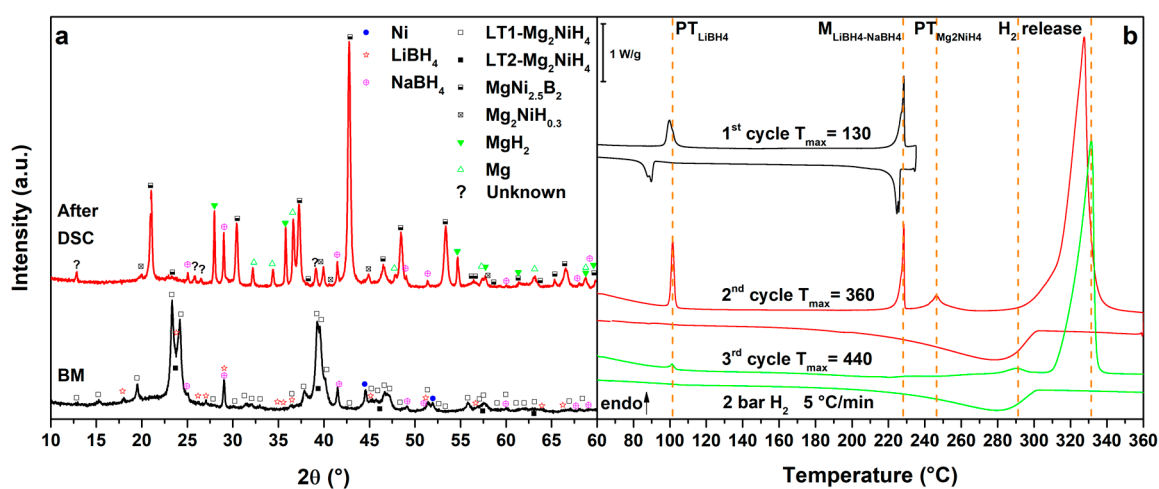


Figure 3. (a) PXD of the ball milled MgNiLiNa (black, down) and after cycling in HP-DSC (red, up); (b) HP-DSC cycling of MgNiLiNa at 5 °C/min under a static pressure of 2.2 bar of H_2 .

3.5. $\text{Mg}_2\text{NiH}_4\text{-LiBH}_4\text{-NaBH}_4$ Eutectic Composition

Figure 4 presents the results obtained for the MgNiLiNa system. Upon heating in the 1st cycle (Figure 4b, 1st cycle), we observe the polymorphic transition of LiBH_4 at $T_{\text{peak}} = 98$ °C, stabilized for the presence of NaBH_4 [36] and the melting of the LiNa eutectic at $T_{\text{peak}} = 228$ °C. Both phase transformations are reversible and slightly undercooled on cooling. In the 2nd cycle (Figure 4b, 2nd cycle), after the previous phase transformations, also the polymorphic transition of Mg_2NiH_4 is observed at $T_{\text{peak}} = 246$ °C, followed by the main hydrogen release from the RHC mixture at $T_{\text{peak}} = 327$ °C under 2.7 bar H_2 . The RHC mixture decomposes similarly to the MgNiLiK system and, on cooling, Mg_2Ni and Mg are hydrogenated to form $\text{Mg}_2\text{NiH}_{0.3}$ and MgH_2 below 302 °C. In the 3rd cycle (Figure 4b, 3rd cycle), previous transitions from LiNa and Mg_2NiH_4 are hardly visible, confirming their decomposition. In fact, the hydrogen release from $\text{Mg}_2\text{NiH}_{0.3}$ and MgH_2 are observed at $T_{\text{peak}} = 290$ °C and 331 °C, respectively. No improvement in the hydrogenation of Mg can be seen on cooling in the 3th cycle. In comparison to the starting components, the hydrogen release temperature of the RHC mixture has not been lowered by the substitution of KBH_4 with NaBH_4 .

The decomposition products of the MgNiLiNa system are similar to those of MgNiLiK , as evidenced by the PXD analysis (Figure 4a, after DSC). Even in this case, the most stable NaBH_4 borohydride is still present after thermal cycling.

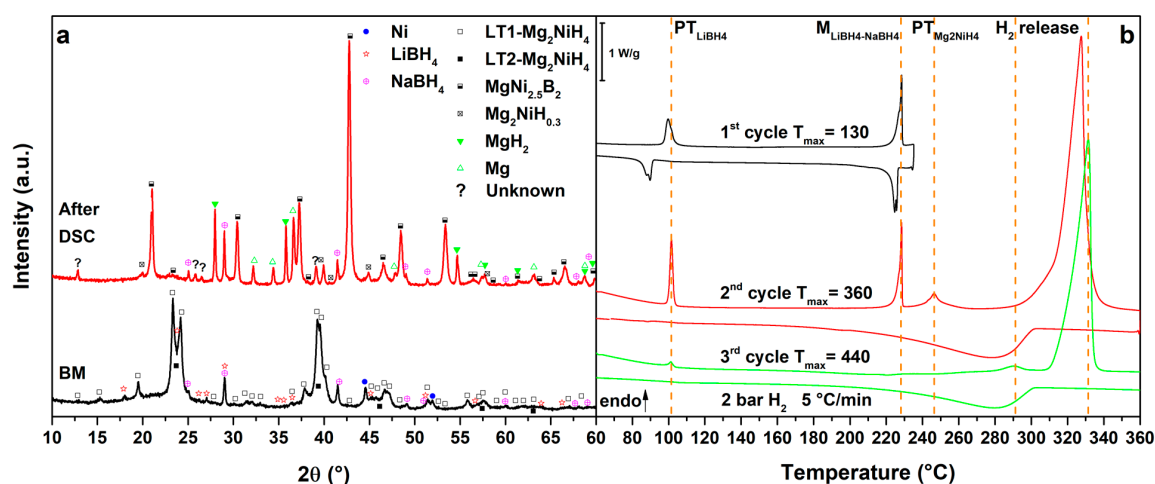


Figure 4. (a) PXD of the ball milled MgNiLiNa (black, down) and after cycling in HP-DSC (red, up); (b) HP-DSC cycling of MgNiLiNa at 5 °C/min under a static pressure of 2.2 bar of H₂.

3.6. Mg₂NiH₄–LiBH₄–Mg(BH₄)₂ Eutectic Composition

Results obtained for the MgNiLiMg system are shown in Figure 5. In the 1st cycle (Figure 5b, 1st cycle), the polymorphic transition of LiBH₄ is observed as a broad peak at T_{peak} = 111 °C, followed by the melting of the eutectic at T_{peak} = 176 °C. Upon cooling the crystallization of the eutectic is not clearly detected, possibly because some Mg(BH₄)₂ has already reacted, enriching the LiBH₄ fraction in the composition of the borohydride mixture [16–18]. In fact, the DSC peak due to the LiBH₄ phase transformation appears more intense on cooling with respect to that observed on heating. Consequently, in the 2nd cycle (Figure 5b, 2nd cycle), the polymorphic transition of LiBH₄ is more defined and the LiMg eutectic melting is hardly detected as a broad peak. At higher temperatures, the Mg₂NiH₄ polymorphic transition is detected at T_{peak} = 246 °C, together with a small peak of hydrogen release from the liquid borohydride, as previously observed in the literature [20]. Furthermore, the main hydrogen release from the RHC mixture starts above 290 °C under 2.7 bar H₂ (T_{peak} = 336 °C). In this temperature range, the decomposition of Mg(BH₄)₂ is also expected [9]. On the other hands, after the decomposition of the mixture, MgNi_{2.5}B₂ and Mg are expected to be formed, so that the decomposition of Mg(BH₄)₂ to Mg, B and H₂ is limited. Upon cooling in the 2nd cycle, a broad hydrogenation peak is observed at T_{peak} = 260 °C related to the formation of MgH₂. Actually, in the 3rd cycle (Figure 5b, 3rd cycle), no peaks related to LiBH₄ or Mg₂NiH₄ phase transformations are observed but several peaks related to hydrogen release can be observed above 231 °C, in a complex multi-steps reaction (T_{peak} = 302 °C, 315 °C and 323 °C). These peaks are related to the full decomposition of residual Mg(BH₄)₂ [9], together with hydrogen release from Mg₂NiH_{0.3} and MgH₂. Hydrogenation of Mg₂Ni and Mg is clearly observed upon cooling below 300 °C. Finally, in the 4th cycle (Figure 5b, 4th cycle), only hydrogen release peaks from Mg₂NiH_{0.3} (T_{peak} = 293 °C) and MgH₂ (T_{peak} = 317 °C) are observed and, during cooling, a peak related to hydrogenation can be detected again below 297 °C.

The decomposition products detected in the PXD pattern after thermal cycling (Figure 5a, after DSC) are always the same, as observed for the MgNiLiK and MgNiLiNa systems. However, in this case, no traces of residual borohydrides are observed, suggesting the full reaction of Mg(BH₄)₂. It is worth to note that the intensity of the diffraction peaks of the unknown phase are higher with respect to the previous systems. The high content of Mg and B in this system suggests that the unknown phase could be related to the Mg–Ni–B system.

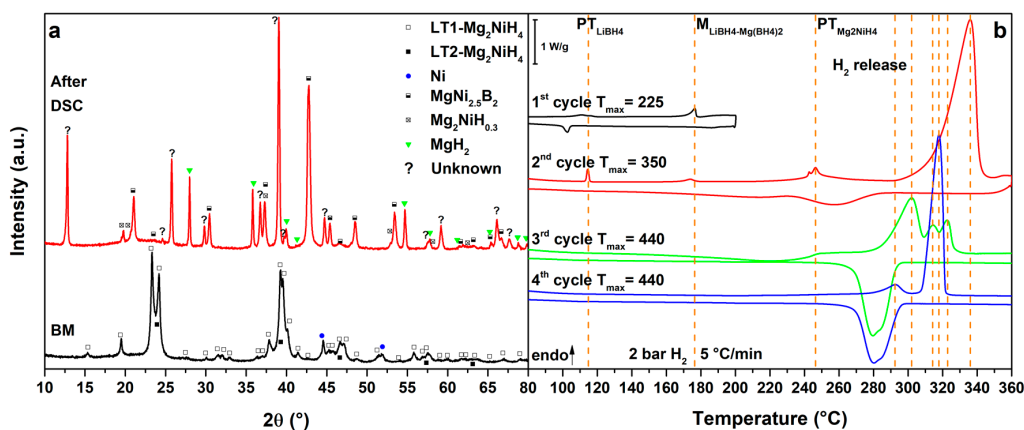


Figure 5. (a) PXD of the ball milled MgNiLiMg (black, down) and after cycling in HP-DSC (red, up); (b) HP-DSC cycling of MgNiLiMg at 5 °C/min under a static pressure of 2.2 bar of H₂.

3.7. Mg₂NiH₄–LiBH₄–Ca(BH₄)₂ Eutectic Composition

Finally, the results obtained for the MgNiLiCa system are reported in Figure 6. The DSC trace of the 1st cycle (Figure 6b, 1st cycle) presents the polymorphic transition of LiBH₄ at $T_{\text{peak}} = 115$ °C, the polymorphic transition of Ca(BH₄)₂ at $T_{\text{peak}} = 150$ °C and the melting of the LiCa eutectic at $T_{\text{peak}} = 202$ °C. Only the polymorphic transition of Ca(BH₄)₂ cannot be observed by DSC on cooling, because of sluggish kinetics [21]. In the 2nd cycle (Figure 6b, 2nd cycle), all the previous transitions of the LiCa system are observed. At higher temperatures, the polymorphic transition of Mg₂NiH₄ is detected at $T_{\text{peak}} = 243$ °C, together with a small peak of hydrogen release from the liquid borohydride, as previously observed in the MgNiLiMg system and in the literature [37]. Furthermore, a DSC endothermic peak due to hydrogen release starts above 300 °C ($T_{\text{peak}} = 332$ °C), under 2.7 bar H₂, so that heating has been stopped at 350 °C, in order to separate hydrogen release reactions. The DSC exothermic DSC peaks due to hydrogenation reactions of Mg₂Ni and Mg can be observed on cooling below 304 °C. In the 3rd cycle (Figure 6b, 3rd cycle), no peaks from the LiCa system are observed, suggesting the occurrence of reactions between Mg₂NiH₄ and the borohydride mixture in the previous cycle. A DSC peak at $T_{\text{peak}} = 298$ °C is clearly related to the hydrogen release from Mg₂NiH_{0.3}, followed by the decomposition of MgH₂ and, at higher temperatures, by the decomposition of Ca(BH₄)₂ to CaH₂ up to 440 °C. In fact, in the 4th cycle (Figure 6b, 4th cycle), the decomposition of the Mg₂NiH_{0.3} is hardly observed but the decomposition of MgH₂ is clearly occurring at $T_{\text{peak}} = 335$ °C. During cooling, a broad peak of hydrogenation can be detected below 304 °C both in the 3rd and 4th cycle.

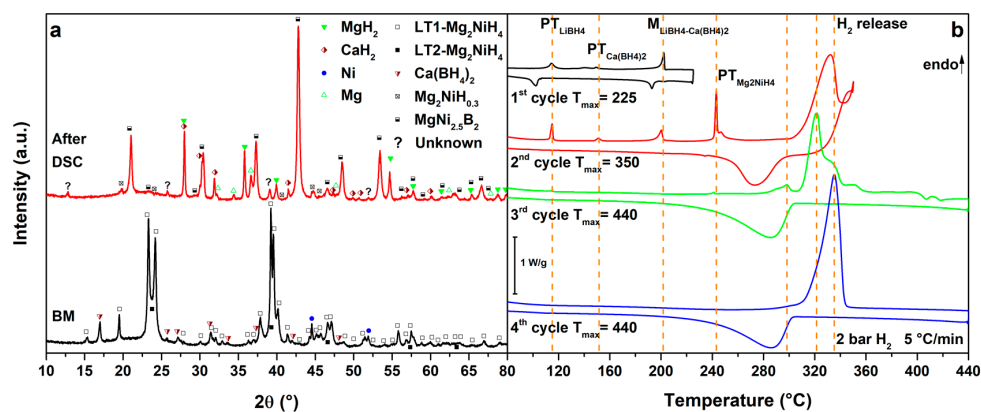


Figure 6. (a) PXD of the ball milled MgNiLiCa (black, down) and after cycling in HP-DSC (red, up); (b) HP-DSC cycling of MgNiLiCa at 5 °C/min under a static pressure of 2.2 bar of H₂.

All the systems investigated in this work present the decomposition of borohydrides from the liquid state, which appears to play a role on the temperature of decomposition of the RHC mixtures. When only LiBH_4 is present, the decomposition peak is at a slightly higher temperature with respect to RHC mixtures containing eutectic borohydrides mixtures, though it does not change significantly in all different systems. When a highly stable borohydride (i.e., NaBH_4 and KBH_4) is present in the eutectic mixture, only LiBH_4 plays an active role in the mixture and the RHC mixture does not decompose completely, so that the stable borohydride is still present in the decomposition products after thermal cycling. On the other hand, if an alkali-earth borohydride (i.e., $\text{Mg}(\text{BH}_4)_2$ and $\text{Ca}(\text{BH}_4)_2$) is mixed with LiBH_4 to form a eutectic, the liquid phase fully decomposes, namely at lower temperatures compared to the pure eutectic mixture alone but complex multi-step reactions are taking place.

In all systems, when the borohydrides and the Mg_2NiH_4 decompose, they always react to form $\text{MgNi}_{2.5}\text{B}_2$ and Mg . The presence of an unknown decomposition product has also been observed in all RHC mixtures with eutectic borohydride mixtures. The low backpressure applied in this case is not high enough to form back the starting borohydrides, though it is able to hydrogenate the decomposed Mg_2Ni and Mg to form $\text{Mg}_2\text{NiH}_{0.3}$ and MgH_2 .

Decomposition temperatures in investigated systems have not been lowered significantly compared to previous studies of Mg_2NiH_4 - MBH_4 mixtures. In fact, the hydrogen release temperature is still far from ambient conditions. A full rehydrogenation has not been obtained because of the limited H_2 pressure applied in the experimental conditions. As for previous studied mixtures [27–31], a hydrogen pressure of 100 bar is expected to fully rehydrogenate the systems. The nanoconfinement of the studied mixtures into a nanoporous scaffold to obtain nanostructured materials [13,15,19,20,22–25,31,32] might be explored to improve the thermodynamics and kinetics of hydrogen sorption reactions and cyclability.

5. Conclusions

In this study RHC systems obtained by mixing Mg_2NiH_4 and eutectic mixtures of borohydrides have been investigated, to explore possible improvements in hydrogen release properties of those systems.

In the investigated RHC mixtures, when LiBH_4 is in eutectic mixture with borohydrides that contain stable single charged metal cation, a slight improvement in the decomposition temperature of the RHC mixture is observed but a leftover of the more stable borohydrides is detected after cycling.

The presence of double charged metal cation in the eutectic mixture causes a full decomposition of the borohydrides in complex multi-step reactions. The presence of a stable liquid at low temperature promotes the decrease of the hydrogen release temperature, if compared to that of pure Mg_2NiH_4 .

Acknowledgments: European Marie Curie Actions under ECOSTORE grant agreement No. 607040 is acknowledged for supporting this work.

Author Contributions: E.M.D. and M.B. conceived and designed the experiments; E.M.D. and S.V. performed the experiments and analysed the data; C.P. and M.D. contributed with materials and fruitful discussion of the results, E.M.D. and M.B. wrote the paper.

Conflicts of Interest: The authors declare no conflict of interest.

References

1. Callini, E.; Atakli, Z.Ö.K.; Hauback, B.C.; Orimo, S.; Jensen, C.; Dornheim, M.; Grant, D.; Cho, Y.W.; Chen, P.; Hjörvarsson, B.; et al. Complex and liquid hydrides for energy storage. *Appl. Phys. A* **2016**, *122*, 353. [[CrossRef](#)]
2. Dornheim, M. Thermodynamics of metal hydrides: Tailoring reaction enthalpies of hydrogen storage materials. In *Thermodynamics—Interaction Studies—Solids, Liquids and Gases*; InTech: Rijeka, Croatia, 2011; pp. 891–918.
3. Martínez-Coronado, R.; Retuerto, M.; Torres, B.; Martínez-Lope, M.J.; Fernández-Díaz, M.T.; Alonso, J.A. High-pressure synthesis, crystal structure and cyclability of the Mg_2NiH_4 hydride. *Int. J. Hydrogen Energy* **2013**, *38*, 5738–5745. [[CrossRef](#)]

4. Noréus, D. Properties of formal low-valence transition metal—hydrogen complexes in Mg_2NiH_4 and Na_2PdH_2 . *Z. Phys. Chem.* **1989**, *163*, 575–578. [[CrossRef](#)]
5. Čermák, J.; Král, L.; David, B. Hydrogen diffusion in Mg_2NiH_4 intermetallic compound. *Intermetallics* **2008**, *16*, 508–517. [[CrossRef](#)]
6. Zeng, K.; Klassen, T.; Oelerich, W.; Bormann, R. Thermodynamic analysis of the hydriding process of Mg-Ni alloys. *J. Alloys Compd.* **1999**, *283*, 213–224. [[CrossRef](#)]
7. Révész, Á.; Gajdics, M.; Schafner, E.; Calizzi, M.; Pasquini, L. Dehydrogenation-hydrogenation characteristics of nanocrystalline Mg_2Ni powders compacted by high-pressure torsion. *J. Alloys Compd.* **2017**, *702*, 84–91. [[CrossRef](#)]
8. Paskevicius, M.; Jepsen, L.H.; Schouwink, P.; Černý, R.; Ravnsbæk, D.B.; Filinchuk, Y.; Dornheim, M.; Besenbacher, F.; Jensen, T.R. Metal borohydrides and derivatives—Synthesis, structure and properties. *Chem. Soc. Rev.* **2017**, *46*, 1565–1634. [[CrossRef](#)] [[PubMed](#)]
9. Paskevicius, M.; Ley, M.B.; Sheppard, D.A.; Jensen, T.R.; Buckley, C.E. Eutectic melting in metal borohydrides. *Phys. Chem. Chem. Phys.* **2013**, *15*, 19774. [[CrossRef](#)] [[PubMed](#)]
10. Nielsen, T.K.; Besenbacher, F.; Jensen, T.R. Nanoconfined hydrides for energy storage. *Nanoscale* **2011**, *3*, 2086. [[CrossRef](#)] [[PubMed](#)]
11. Rude, L.H.; Nielsen, T.K.; Ravnsbæk, D.B.; Bösenberg, U.; Ley, M.B.; Richter, B.; Arnbjerg, L.M.; Dornheim, M.; Filinchuk, Y.; Besenbacher, F.; et al. Tailoring properties of borohydrides for hydrogen storage: A review. *Phys. Status Solidi (a)* **2011**, *208*, 1754–1773. [[CrossRef](#)]
12. Dematteis, E.M.; Pinatel, E.R.; Corno, M.; Jensen, T.R.; Baricco, M. Phase diagrams of the $LiBH_4$ – $NaBH_4$ – KBH_4 system. *Phys. Chem. Chem. Phys.* **2017**, *19*, 25071–25079. [[CrossRef](#)] [[PubMed](#)]
13. Roedern, E.; Hansen, B.R.S.; Ley, M.B.; Jensen, T.R. Effect of Eutectic Melting, Reactive Hydride Composites and Nanoconfinement on Decomposition and Reversibility of $LiBH_4$ – KBH_4 . *J. Phys. Chem. C* **2015**, *119*, 25818–25825. [[CrossRef](#)]
14. Liu, Y.; Reed, D.; Paterakis, C.; Contreras Vasquez, L.; Baricco, M.; Book, D. Study of the decomposition of a 0.62 $LiBH_4$ –0.38 $NaBH_4$ mixture. *Int. J. Hydrogen Energy* **2017**, *42*, 22480–22488. [[CrossRef](#)]
15. Javadian, P.; Sheppard, D.A.; Buckley, C.E.; Jensen, T.R. Hydrogen storage properties of nanoconfined $LiBH_4$ – $NaBH_4$. *Int. J. Hydrogen Energy* **2015**, *40*, 14916–14924. [[CrossRef](#)]
16. Liu, X.; Peaslee, D.; Sheehan, T.P.; Majzoub, E.H. Decomposition behaviour of eutectic $LiBH_4$ – $Mg(BH_4)_2$ and its confinement effects in ordered nanoporous carbon. *J. Phys. Chem. C* **2014**, *118*, 27265–27271. [[CrossRef](#)]
17. Fang, Z.-Z.; Kang, X.-D.; Wang, P.; Li, H.-W.; Orimo, S.-I. Unexpected dehydrogenation behaviour of $LiBH_4$ / $Mg(BH_4)_2$ mixture associated with the in situ formation of dual-cation borohydride. *J. Alloys Compd.* **2010**, *491*, L1–L4. [[CrossRef](#)]
18. Bardají, E.G.; Zhao-Karger, Z.; Boucharat, N.; Nale, A.; van Setten, M.J.; Lohstroh, W.; Röhm, E.; Catti, M.; Fichtner, M. $LiBH_4$ – $Mg(BH_4)_2$: A physical mixture of metal borohydrides as hydrogen storage material. *J. Phys. Chem. C* **2011**, *115*, 6095–6101. [[CrossRef](#)]
19. Zhao-Karger, Z.; Witter, R.; Bardaji, E.G.; Wang, D.; Cossement, D.; Fichtner, M. Altered reaction pathways of eutectic $LiBH_4$ – $Mg(BH_4)_2$ by nanoconfinement. *J. Mater. Chem. A* **2013**, *1*, 3379. [[CrossRef](#)]
20. Javadian, P.; Jensen, T.R. Enhanced hydrogen reversibility of nanoconfined $LiBH_4$ – $Mg(BH_4)_2$. *Int. J. Hydrogen Energy* **2014**, *39*, 9871–9876. [[CrossRef](#)]
21. Lee, J.Y.; Ravnsbæk, D.B.; Lee, Y.S.; Kim, Y.; Cerenius, Y.; Shim, J.; Jensen, T.R.; Hur, N.H.; Cho, Y.W. Decomposition reactions and reversibility of the $LiBH_4$ – $Ca(BH_4)_2$ composite. *J. Phys. Chem. C* **2009**, *113*, 15080–15086. [[CrossRef](#)]
22. Lee, Y.-S.; Filinchuk, Y.; Lee, H.S.; Suh, J.-Y.; Kim, J.W.; Yu, J.-S.; Cho, Y.W. On the Formation and the Structure of the First Bimetallic Borohydride Borate, $LiCa_3(BH_4)(BO_3)_2$. *J. Phys. Chem. C* **2011**, *115*, 10298–10304. [[CrossRef](#)]
23. Ampoumogli, A.; Charalambopoulou, G.; Javadian, P.; Richter, B.; Jensen, T.R.; Steriotis, T. Hydrogen desorption and cycling properties of composites based on mesoporous carbons and a $LiBH_4$ – $Ca(BH_4)_2$ eutectic mixture. *J. Alloys Compd.* **2015**, *645*, S480–S484. [[CrossRef](#)]
24. Javadian, P.; Sheppard, D.A.; Buckley, C.E.; Jensen, T.R. Hydrogen storage properties of nanoconfined $LiBH_4$ – $Ca(BH_4)_2$. *Int. J. Hydrogen Energy* **2015**, *11*, 96–103. [[CrossRef](#)]

25. Lee, H.S.; Hwang, S.-J.; Kim, H.K.; Lee, Y.-S.; Park, J.; Yu, J.-S.; Cho, Y.W. In Situ NMR Study on the Interaction between $\text{LiBH}_4\text{-Ca}(\text{BH}_4)_2$ and Mesoporous Scaffolds. *J. Phys. Chem. Lett.* **2012**, *3*, 2922–2927. [[CrossRef](#)] [[PubMed](#)]
26. Chaudhary, A.-L.; Li, G.; Matsuo, M.; Orimo, S.; Deledda, S.; Sørby, M.H.; Hauback, B.C.; Pistidda, C.; Klassen, T.; Dornheim, M. Simultaneous desorption behaviour of M borohydrides and Mg_2FeH_6 reactive hydride composites (M = Mg, then Li, Na, K, Ca). *Appl. Phys. Lett.* **2015**, *107*, 073905. [[CrossRef](#)]
27. Vajo, J.J.; Li, W.; Liu, P. Thermodynamic and kinetic destabilization in $\text{LiBH}_4/\text{Mg}_2\text{NiH}_4$: Promise for borohydride-based hydrogen storage. *Chem. Commun.* **2010**, *46*, 6687–6689. [[CrossRef](#)] [[PubMed](#)]
28. Li, W.; Vajo, J.J.; Cumberland, R.W.; Liu, P.; Hwang, S.-J.; Kim, C.; Bowman, R.C. Hydrogenation of magnesium nickel boride for reversible hydrogen storage. *J. Phys. Chem. Lett.* **2010**, *1*, 69–72. [[CrossRef](#)]
29. Afonso, G.; Bonakdarpour, A.; Wilkinson, D.P. Hydrogen storage properties of the destabilized $4\text{NaBH}_4/5\text{Mg}_2\text{NiH}_4$ composite system. *J. Phys. Chem. C* **2013**, *117*, 21105–21111. [[CrossRef](#)]
30. Bergemann, N.; Pistidda, C.; Milanese, C.; Emmeler, T.; Karimi, F.; Chaudhary, A.-L.; Chierotti, M.R.; Klassen, T.; Dornheim, M. $\text{Ca}(\text{BH}_4)_2\text{-Mg}_2\text{NiH}_4$: On the pathway to a $\text{Ca}(\text{BH}_4)_2$ system with a reversible hydrogen cycle. *Chem. Commun.* **2016**, *52*, 4836–4839. [[CrossRef](#)] [[PubMed](#)]
31. Javadian, P.; Zlotea, C.; Ghimbeu, C.M.; Latroche, M.; Jensen, T.R. Hydrogen storage properties of nanoconfined $\text{LiBH}_4\text{-Mg}_2\text{NiH}_4$ Reactive Hydride Composites. *J. Phys. Chem. C* **2015**, *119*, 5819–5826. [[CrossRef](#)]
32. Ley, M.B.; Roedern, E.; Jensen, T.R. Eutectic melting of $\text{LiBH}_4\text{-KBH}_4$. *Phys. Chem. Chem. Phys.* **2014**, *16*, 24194–24199. [[CrossRef](#)] [[PubMed](#)]
33. Blomqvist, H.; Noréus, D. Mechanically reversible conductor–insulator transition in Mg_2NiH_4 . *J. Appl. Phys.* **2002**, *91*, 5141–5148. [[CrossRef](#)]
34. Polanski, M.; Nielsen, T.K.; Kunce, I.; Norek, M.; Płociński, T.; Jaroszewicz, L.R.; Gundlach, C.; Jensen, T.R.; Bystrzycki, J. Mg_2NiH_4 synthesis and decomposition reactions. *Int. J. Hydrogen Energy* **2013**, *38*, 4003–4010. [[CrossRef](#)]
35. El Kharbachi, A.; Pinatel, E.R.; Nuta, I.; Baricco, M. A thermodynamic assessment of LiBH_4 . *Calphad* **2012**, *39*, 80–90. [[CrossRef](#)]
36. Dematteis, E.M.; Roedern, E.; Pinatel, E.R.; Corno, M.; Jensen, T.R.; Baricco, M. A thermodynamic investigation of the $\text{LiBH}_4\text{-NaBH}_4$ system. *RSC Adv.* **2016**, *6*, 60101–60108. [[CrossRef](#)]
37. Javadian, P.; GharibDoust, S.P.; Li, H.-W.; Sheppard, D.A.; Buckley, C.E.; Jensen, T.R. Reversibility of LiBH_4 facilitated by the $\text{LiBH}_4\text{-Ca}(\text{BH}_4)_2$ eutectic. *J. Phys. Chem. C* **2017**, *121*, 18439–18449. [[CrossRef](#)]



© 2018 by the authors. Licensee MDPI, Basel, Switzerland. This article is an open access article distributed under the terms and conditions of the Creative Commons Attribution (CC BY) license (<http://creativecommons.org/licenses/by/4.0/>).